J|A|C|S
ARTICLES
Published on Web 03/01/2007

Counterion, Temperature, and Time Modulation of Nanometric Chiral Ribbons from Gemini-Tartrate Amphiphiles

Aurélie Brizard,[†] Carole Aimé,[†] Thomas Labrot,[†] Ivan Huc,[†] Damien Berthier,[†] Franck Artzner,[‡] Bernard Desbat,[§] and Reiko Oda*[,†]

Contribution from the Institut Européen de Chimie et Biologie, 2 rue Robert Escarpit, 33607 Pessac cedex, France, UMR-CNRS 6626 Bât 11A Université de Rennes I, Campus Beaulieu, 35042 Rennes cedex, France, and Laboratoire de Physico-Chimie Moléculaire, 351 cours de la libération, 33405 Talence, France

Received November 16, 2006; E-mail: r.oda@iecb.u-bordeaux.fr

Abstract: Amphiphile supramolecular assemblies result from the cooperative effects of multiple weak interactions between a large number of subcomponents. As a result, prediction of and control over the morphologies of such assemblies remains difficult to achieve. Here, we described the fine-tuning of the shape, size, and morphology transitions of twisted and helical membranes formed by non-chiral dicationic *n*-2-*n* gemini amphiphiles complexed with chiral tartrate anions. We have reported that such systems express the chirality of the tartrate components at a supramolecular level and that the mechanism of the chiral induction by counterions involves specific anion cation recognition and the induction of conformationally labile chirality in the cations. Here, we demonstrate that the morphologies and dimensions of twisted and helical ribbons, as well as tubules, can be controlled and that interconversion between these structures can be induced upon modifying temperature, upon introducing small amounts of additives, or slightly modifying molecular structure. Specifically, electron microscopy, IR spectroscopy, and small-angle X-ray scattering show that (i) varying the hydrophobic chain length or adding gemini having bromide counterions (1%) or the opposite enantiomer (10%) leads to an increase of the diameter of membrane tubules from 33 to 48.5 nm; (ii) further addition (1.5%) of gemini bromide or a slight increase in temperature induces a transition from tubules to twisted ribbons; (iii) the twist pitch of the ribbons can be continuously tuned by varying enantiomeric excess; and (iv) it was also observed that the morphologies of these ribbons much evolve with time. Such unprecedented observations over easy tuning of the chiral supramolecular structures are clearly related to the original feature that the induction of chirality is solely due the counterions, which are much more mobile than the amphiphiles.

Introduction

Chirality and Fiber Morphology. Chiral amphiphilic molecules often assemble in solution to form aggregates with high aspect ratios such as rods, tapes, or tubes, suggesting that chirality is intimately associated with the growth and stability of self-assembled fibers of small organic molecules.[1] Often, but not always, chirality is expressed in the morphology of these fibers at a supramolecular scale of nanometers to micrometers;[2] the fibrous structures may be coiled, twisted, or wound around one another and exist as a left-handed or a right-handed form. These intriguing shapes can be simply visualized by microscopic techniques and have fascinated both chemists and physicists. On fundamental grounds, the relationship between molecular chirality (scale ~Å) and supramolecular chirality (scale ~μm) as expressed in these structures represents an excellent model for studying the emergence of specific shapes at a macroscopic scale through cooperative interactions between a large number of very small building blocks. In addition to this fundamental aspect, chiral fibrous objects possess a great potential for applications in the development of new functional supramolecular devices, taking advantage of the chirality of the molecular constituents organized in a hierarchical manner and/or of the supramolecular chirality of the fibers that can be generated. Among those applications are chiral recognition using chiral fibers, using chiral fibers as templates for helical crystallization of proteins, or the growth of inorganic replicas, as is summarized elsewhere.[1]

In a majority of cases, the handedness of a chiral self-assembled fiber is controlled by the stereochemistry of the molecule. One enantiomer gives a right-handed fiber and the other enantiomer a left-handed fiber. There are, however, some exceptions, as when a pure enantiomer gives a mixture of right- and left-handed helices,[3] or when the handedness depends on external parameters such as the cooling rate.[4]

[†] Institut Européen de Chimie et Biologie.
[‡] Université de Rennes I.
[§] Laboratoire de Physico-Chimie Moléculaire.

(1) For a review on chiral fibrous structures, see: (a) Ihara, H.; Takafuji, M.; Sakurai, T. In *Encyclopedia of Nanoscience and Nanotechnology*; Nalwa, H. S., Ed.; American Scientific Publishers: 2004; Vol. 9, pp 473−495. (b) Brizard, A.; Oda, R.; Huc, I. *Top. Curr. Chem.* **2005**, *256*, 167.

(2) A vast number of reports deal with chiral supramolecular structures. Here, we mainly focus on small amphiphilic molecules.

10.1021/ja0682172 CCC: $37.00

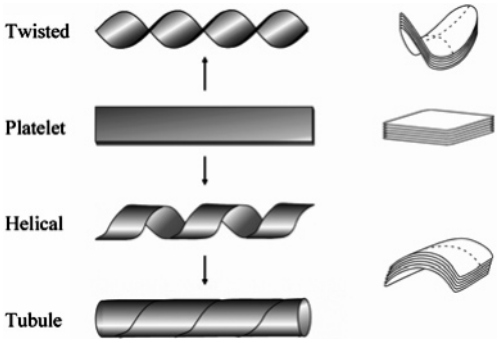

Figure 1. Schematic representation of twisted ribbons having saddle-like curvature versus helical ribbons and tubules with cylindrical curvature.

Among the variety of chiral fibrillar structures encountered in the literature, probably the most commonly described are chiral ribbons of single or multiple bilayer membranes. Such ribbons can be classified into two different morphologies: helical and twisted shapes (Figure 1). Helical ribbons have a cylindrical curvature and can be precursors of tubules (see below). For example, helical ribbons were obtained with diacetylenic lipids,[5] *N*-octyl-l-galactonamide,[6] cytidine myristoylphosphatidyl conjugates,[7] and some chiral single-chain ammonium amphiphiles.[8] Tubules form using diacetylenic lipids,[9] glycolipids,[10,11] and some steroids.[12] Detailed reviews can be found elsewhere.[13]

In contrast, twisted ribbons have Gaussian or saddle-like curvature. Typical examples of twisted morphologies are those of hydrostearic acid,[14] of double-chain ammonium amphiphiles derived from glutamic acid,[15] or of diammonium cationic gemini surfactants.[16,17] Why some ribbons have a cylindrical curvature whereas others have a saddle-like shape is still a matter of debate. A theoretical model treating the energy differences in the two types of curvatures has been introduced, and it has been suggested that, for fluid membranes, twisted ribbons are favored, whereas crystalline molecular organization imposes a helical curvature.[18,19] Yet this may not be general and is not always verified at the experimental level.[19,20]

Morphology Control of Chiral Fibers. One of the great challenges in this area is to understand and control the parameters that determine the morphology of chiral assemblies. Very often, the balance between these parameters is subtle; seemingly slight changes in the experimental conditions such as the nature of the solvent or the age of the sample may lead to important changes of chiral fiber morphology. Fiber formation is generally a kinetically controlled event. It has been observed that tubules grow from helical ribbons[7,21] and the size of the tubules[22] or even the handedness of the helices varies with the cooling rate.[4]

In addition to these environmental parameters, the most critical factor is the molecular structure of the amphiphile, within which very slight changes may lead to completely different aggregate morphologies. Typical molecular parameters that induce significant morphology variation are the length[4,23−25] and the number of unsaturations[20] of alkyl chains. In the case of bolaamphiphiles, not only the length of the spacer alkyl group matters but also whether it has an odd or an even number of carbon atoms, as revealed by IR spectroscopy.[26−28] With the salts of L- and D-12-hydroxystearic acid, the nature of the cation was reported to affect helix handedness.[29]

Additives or mixtures of different molecules in various proportions have also been used to tune chiral aggregate morphologies. For example, a transition from twisted ribbons to helical ribbons has been observed in mixtures of cardanyl glucosides with saturated and unsaturated alkyl chains.[20] The diameter of tubules formed by diacetylenic lipid can be modified by a slight structural change,[30] upon adding short-chain phos-

(3) (a) Lin, Y.-C.; Kachar, B.; Weiss, R. G. *J. Am. Chem. Soc.* **1989**, *111*, 5542. (b) Thomas, B. N.; Corcoran, R. C.; Cotant, C. L.; Lindemann, C. M.; Kirsch, J. E.; Persichini, P. J. *J. Am. Chem. Soc.* **1998**, *120*, 12178. (c) Thomas, B. N.; Lindemann, C. M.; Clark, N. A. *Phys. Rev. E* **1999**, *59*, 3040. (d) Thomas, B. N.; Lindemann, C. M.; Corcoran, R. C.; Cotant, C. L.; Kirsch, J. E.; Persichini, P. J. *J. Am. Chem. Soc.* **2002**, *124*, 1227. (e) Zastavker, Y. V.; Asherie, N.; Lomakin, A.; Pande, J.; Donovan, J. M.; Schnur, J. M.; Benedek, G. B. *Proc. Natl. Acad. Sci. U.S.A.* **1999**, *96*, 7883. (f) Pakhomov, S.; Hammer, R. P.; Mishra, B. K.; Thomas, B. N. *Proc. Natl. Acad. Sci. U.S.A.* **2003**, *100*, 3040.
(4) Murata, K.; Aoki, M.; Suzuki, T.; Harada, T.; Kawabata, H.; Komori, T.; Ohseto, F.; Ueda, K.; Shinkai, S. *J. Am. Chem. Soc.* **1994**, *116*, 6664.
(5) (a) Schnur, J. M. *Science* **1993**, *262*, 1669. (b) Yager, P.; Schoen, P. E. *Mol. Cryst. Liq. Cryst.* **1984**, *106*, 371. (c) Schnur, J. M.; Ratna, B. R.; Selinger, J. V.; Singh, A.; Jyothi, G.; Easwaran, K. R. K. *Science* **1994**, *264*, 945.
(6) Fuhrhop, J.-H.; Schnieder, P.; Boekema, E.; Helfrich, W. *J. Am. Chem. Soc.* **1988**, *110*, 2861.
(7) Yanagawa, H.; Ogawa, Y.; Furuta, H.; Tsuno, K. *J. Am. Chem. Soc.* **1989**, *111*, 4567.
(8) Kunitake, T.; Yamada, N. *Chem. Commun.* **1986**, 655.
(9) (a) Spector, M. S.; Easwaran, K. R. K.; Jyothi, G.; Selinger, J. V.; Singh, A.; Schnur, J. M. *Proc. Natl. Acad. Sci. U.S.A.* **1996**, *93*, 12943. (b) Spector, M. S.; Selinger, J. V.; Schnur, J. M. *J. Am. Chem. Soc.* **1997**, *119*, 8533. (c) Spector, M. S.; Selinger, J. V.; Singh, A.; Rodriguez, J. M.; Price, R. R.; Schnur, J. M. *Langmuir* **1998**, *14*, 3493. (d) Douliez, J.-P.; Lavenant, L.; Renard, D. J. *Colloid Interface Sci.* **2003**, *266*, 477. (e) Spector, M. S.; Price, C. E.; Schnur, J. M. *Adv. Mater.* **1999**, *11*, 337−340.
(10) (a) Shimizu, T.; Masuda, M.; Minamikawa, H. *Chem. Rev.* **2005**, *105*, 1401. (b) Zhu, H.; John, G.; Wei, B. *Chem. Phys. Lett.* **2005**, *405*, 49. (c) Blanzat, M.; Massip, S.; Speziale, V.; Perez, E.; Rico-Lattes, I. *Langmuir* **2001**, *17*, 3512. (d) Kamiya, S.; Minamikawa, H.; Jong, H. J.; Bo, Y.; Mitsutoshi, M.; Shimizu, T. *Langmuir* **2005**, *21*, 743.
(11) Masuda, M.; Shimizu, T. *Langmuir* **2004**, *20*, 5969.
(12) (a) Terech, P.; de Geyer, A.; Struth, B.; Talmon, Y. *Adv. Matter.* **2002**, *14*, 495. (b) Zastavjern, Y. V.; Asherie, N.; Lomakin, A.; Pande, J.; Donovan, J. M.; Schnur, J. M.; Benedek, G. B. *Proc. Natl. Acad. Sci. U.S.A.* **1999**, *96*, 7883.
(13) Shimizu, T.; Masuda, M.; Minamikawa, H. *Chem. Rev.* **2005**, *105*, 1401 and references therein.
(14) (a) Tachibana, T.; Kambara, H. *J. Am. Chem. Soc.* **1965**, *87*, 3015. (b) Tachibana, T.; Kambara, H. *Bull. Chem. Soc. Jpn.* **1969**, *42*, 3422.
(15) Nakashima, N.; Asakuma, S.; Kim, J.-M.; Kunitake, T. *Chem. Lett.* **1984**, 1709.
(16) (a) Oda, R.; Huc, I.; Candau, S. J. *Angew. Chem., Int. Ed.* **1998**, *37*, 2689. (b) Oda, R.; Huc, I.; Candau, S. J.; MacKintosh, F. C. *Nature* **1999**, *399*, 566.
(17) The distinction between twisted and helical chiral morphologies is not always straightforward, and ribbons having both a twisted and a helical component can also form. It should also be mentioned that the terms "helical" versus "ribbons" are not yet the universally defined nomenclatures. Helical ribbons are sometimes called twisted and vice versa.
(18) Jacques, J.; Collet, A.; Wilen, S. H. *Enantiomers, Racemates and Resolutions*, 3rd ed.; Krieger: Malabar, FL, 1994.
(19) (a) Spector, M. S.; Selinger, J. V.; Schnur, J. M. Chiral molecular self-assembly. In *Materials Chirality-Topics in Stereochemistry*; Green, M. M., Nolte, R. J. M., Meijer, E. W., Denmark, S. E., Siegel, J., Eds.; Wiley: Hoboken, NJ, 2003; Vol. 24, Chapter 5. (b) Selinger, J. V.; Spector, M. S.; Schnur, J. M. *J. Phys. Chem. B* **2001**, *105*, 7158.
(20) John, G.; Jung, J. H.; Minamikawa, H.; Yoshida, K.; Shimizu, T. *Chem.-Eur. J.* **2002**, *8*, 5494.
(21) Nakashima, N.; Asakuma, S.; Kunitake, T. *J. Am. Chem. Soc.* **1985**, *107*, 509.
(22) Thomas, B. N.; Safinya, C. R.; Plano, R. J.; Clark, N. A. *Science* **1995**, *267*, 1635.
(23) Yamada, K.; Ihara, H.; Ide, T.; Fukumoto, T.; Hirayama, C. *Chem. Lett.* **1984**, 1713.
(24) Hanabusa, K.; Maesaka, Y.; Kimura, M.; Shirai, H. *Tetrahedron Lett.* **1999**, *40*, 2385.
(25) Becerril, J.; Burguete, M. I.; Escuder, B.; Luis, S. V.; Miravet, J. F.; Querl, M. *Chem. Commun.* **2002**, 738.
(26) Nakazawa, I.; Masuda, M.; Okada, Y.; Hanada, T.; Yase, K.; Asai, M.; Shimizu, T. *Langmuir* **1999**, *15*, 4757.
(27) Shimizu, T.; Masuda, M. *J. Am. Chem. Soc.* **1997**, *119*, 2812.
(28) Schnieder, J.; Messerschmidt, C.; Schulz, A.; Gnade, M.; Schade, B.; Luger, P.; Bombicz, P.; Hubert, V.; Fuhrhop, J.-H. *Langmuir* **2002**, *16*, 8575.
(29) Tachibana, T.; Kayama, S.; Takeno, H. *Bull. Chem. Soc. Jpn.* **1972**, *45*, 415.
(30) Thomas, B. N.; Lindemann, C. M.; Corcoran, R. C.; Cotant, C. L.; Kirshch, J. E.; Persichini, P. J. *J. Am. Chem. Soc.* **2002**, *124*, 1227.

pholipids,[31] upon varying solvents or counterions,[32] or changing the chain length of bolaamphiphiles.[11]

Mixing the two enantiomers generally results in important changes in fiber morphology. Racemates tend to form platelets that do not express any chirality. In a couple of cases,[33] as, for example, for diacetylenic lipid,[34] a mixture of right-handed and left-handed helices is observed instead of platelets. Data are rarely available concerning the behavior of mixtures of enantiomers other than 1:1 racemic mixtures. In the case of diacetylenic lipids,[34b] the phase separation between enantiomers should lead to tubules of opposite handedness, the proportions of which reflect the overall proportion of enantiomers.

Most of these systems are formed with amphiphilic molecules possessing chiral centers, which influence directly the morphologies of the self-assembled structures. In contrast, we have reported a unique system of chiral self-assemblies based on a new concept where non-chiral cationic bis-quaternary ammonium gemini surfactants[35] having the formula C_2H_4-1,2-$((CH_3)_2N^+C_nH_{2n+1})_2$, denoted as *n*-2-*n*, formed twisted multilayered ribbons in solution in the presence of chiral tartrate counter-anions.[16b] The handedness of such ribbons depends on the configuration of the tartrate anions, and the twist pitch decreases continuously with the increase in enantiomeric excess (ee). Such ribbons form a 3D network and gel both water and some organic solvents.[16a] This is so far the only example of induction of supramolecular chirality by chiral counterions in non-chiral amphiphilic molecular systems, where the chirality can be tuned in a continuous manner. We have reported that the mechanism of chiral induction by counterions involves specific anion−cation recognition and the induction of conformationally labile chirality in the cations.[36] Herein, we demonstrate that these gemini amphiphiles do not only form twisted ribbons but also helical ribbons and tubules and that the dimensions of these chiral structures can be finely tuned. Parameters such as temperature, kinetic evolution, stoichiometry, enantiomeric excess, and the presence of minute amounts of additives determine and allow us to control the morphology and the dimensions of the nanometric ribbons in an unprecedented way. For example, replacing 1% of tartrate ions with bromide ions gives rise to a 10 nm increase of the tubule diameter. A unique thermally reversible transition between twisted ribbons and helical tubules is also described.

Experimental Section

Synthesis. *n*-2-*n* Tartrate Synthesis ($n = 14-20$): Ion Exchange. The *n*-2-*n* amphiphiles with bromide counterions were synthesized as previously reported.[37] The procedure for bromide to tartrate exchange as we have previously reported[36] was further optimized to achieve strict stoichiometry. As it is developed in the Results, the presence of residual bromide, even less than 2%, may have a dramatic effect on the properties of the prepared gemini amphiphiles.[38]

Thus, a suspension of the silver salt of tartaric acid in methanol was prepared before each use upon mixing D- or L-tartaric acid and Ag_2CO_3 (1 equiv), followed by vigorous stirring under slight vacuum for 1 h. A hot solution of the *n*-2-*n* surfactant in methanol (1 equiv, typically 50−100 mg scale) was added, and the mixture was stirred for 30 min at 40−50 °C and filtered on Celite to give a colorless solution. After evaporation, the product was dissolved in a mixture of chloroform/methanol (9/1, v/v), precipitated with ether, filtered, and dried. The high yield of ion exchange and the stoichiometry were confirmed by element analysis.

Example of 16-2-16 L-tartrate ^{1}H NMR (400 MHz, $CDCl_3/CD_3OD$ 9/1, 25 °C, δ ppm): 4.23 (s, 2H), 3.92 (dm, 4H, $^2J = 33.88$ Hz, $^3J = 9.16$ Hz), 3.30 (m, 4H), 3.10 (d, 12H, $^3J = 7$ Hz), 1.64 (m, 4H), 1.18−1.29 (m, 50H), 0.81 (t, 6H, $^3J = 6.69$ Hz). ^{13}C NMR (100 MHz, $CDCl_3/CD_3OD$ 9/1, 25 °C, δ ppm): 178.01, 66.10, 51.30, 32.47, 30.70, 30.53, 30.26, 30.20, 30.02, 29.90, 26.75, 23.23, 14.6. Anal. Calcd: C, 67.15; H, 12.08; N, 3.73; O, 17.04. Found: C, 66.82; H, 12.16; N, 3.76; O, 17.34.

Freeze-Fracture Electron Microscopy. Freeze-fracture experiments were performed with a Balzers vacuum chamber BAF 300 (Balzers, Liechtenstein). A small droplet of mixture was sandwiched between two copper specimen holders. The sandwich was then frozen with liquid propane cooled with liquid nitrogen. The frozen sandwich was additionally fixed to a transport unit under liquid nitrogen and transferred to the fracture replication stage in a chamber that was then pumped down to 10^{-6} mbar at −120 °C. Immediately after fracturing, replication took place by first shadowing with platinum/carbon at 45° and then with carbon deposition at 90°. The sample was allowed to warm to room temperature. Replicas were retrieved and cleaned in water and mounted on 200-mesh copper grids.

Transmission Electron Microscopy. Observations were made with a Cryo-electron microscope FEI EM120 (120 kV), and the images were recorded on a Gatan ssCCD camera 2k × 2k.

For the samples that were not freeze fractured, they were fixed by either Pt vapor or negative staining plus Pt vaporization. The aqueous dispersions of the gels (10 mM) were put onto an carbon-coated Cu grid, excess water was blotted with filter paper, and then the sample was negatively stained with uranyl acetate solution (1.5 wt %). For Pt vaporization, the same vacuum chamber used for freeze fracture was used except that the shadowing was done at 11 °C.

FT-IR Spectroscopy Measurements. FT-IR spectra were recorded on a Magna 560 (Nicolet) FT-IR spectrometer equipped with a germanium-coated KBr beam splitter and a HgCdTe (MCT) detector cooled at 77 K. To avoid the intense absorption peak of H_2O, which hides carboxylate resonances, solutions were prepared in D_2O. Generally, 100 scans were added at a resolution of 4 cm^{-1}. The transmission measurements were performed with two ZnSe windows. For the experiments with temperature variation, a homemade heating cell was used associated with a WEST 6100 hot stage temperature controller.

Small-Angle X-ray Scattering. Experimental data were collected on the high brilliance ID2A beamline of the European Synchrotron Radiation Facility (ESRF, Grenoble, France) using X-ray wavelength λ of 0.9995 Å. Small-angle X-ray scattering (SAXS) was collected on an intensified CCD (chip charge-coupled device) with a sample to detector distance of 1.2 m. The X-ray patterns were, therefore, recorded for a range of reciprocal spacing q(Å^{-1}) from 0.022 to 0.5 Å^{-1}. A second image intensified CCD was positioned at an oblique angle (32°) at a distance of about 120 mm to collect simultaneously wide-angle X-ray scattering (WAXS) for a range of reciprocal spacing q(Å^{-1}) from 0.8 to 5 Å^{-1}. All samples exhibited powder diffraction, and the scattering intensities as a function of the radial wave vector, $q = 4\pi/\lambda \sin(\theta)$, were determined by circular integration. The samples were conditioned

(31) Svenson, S.; Messersmith, P. B. *Langmuir* **1999**, *15*, 4464.
(32) Markowitz, M. A.; Schnur, J. M.; Singh, A. *Chem. Phys. Lipids* **1992**, *62*, 193.
(33) (a) Gulik-Krzywicki, T.; Fouquey, C.; Lehn, J.-M. *Proc. Natl. Acad. Sci. U.S.A.* **1993**, *90*, 163. (b) Yamada, N.; Sasaki, T.; Murata, H.; Kunitake, T. *Chem. Lett.* **1989**, 205.
(34) (a) Singh, A.; Burke, T. G.; Calvert, J. M.; Georger, J. H.; Herendeen, B.; Price, R. R.; Schoen, P. E.; Yager, P. *Chem. Phys. Lipids* **1988**, *47*, 135. (b) Spector, M. S.; Selinger, J. V.; Singh, A.; Rodriguez, J. M.; Price, R. R.; Schnur, J. M. *Langmuir* **1998**, *14*, 3493.
(35) For reviews on gemini surfactants, see: (a) Menger, F. M.; Keiper, J. *Angew. Chem., Int. Ed.* **2000**, *39*, 1906−1920. (b) Zana, R., Xia, J., Eds. *Gemini Surfactants*; Marcel Dekker: New York, 2004.
(36) Berthier, D.; Buffeteau, T.; Léger, J.-M.; Oda, R.; Huc, I. *J. Am. Chem. Soc.* **2002**, *124*, 13486.
(37) Oda, R.; Huc, I.; Candau, S. J. *Chem. Commun.* **1997**, 2105.
(38) Brizard, A.; Dolain, C.; Huc, I.; Oda, R. *Langmuir* **2006**, *22*, 3591.

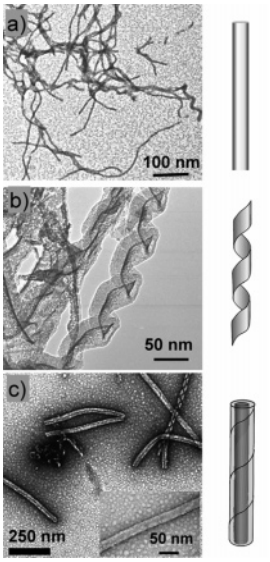

Figure 2. TEM micrographs and schematic representation of the evolution of the morphologies of fibrous structures of 16-2-16 (10 mM in H_2O) with time. (a) Ill-defined fibers are observed after 2 h. (b) These fibers evolved to helical ribbons after 3 h, (c) which closed to form tubules after 36 h.

in 1.4−1.6-mm glass capillaries and introduced into a homemade capillaries holder, which allows maintaining 20 capillaries all together at a controlled temperature or applying a determined temperature program monitored via a computer.[39]

Results

The effect of various parameters on the morphologies of gemini tartrate assemblies was investigated as described below.

Morphology of Ribbons for ee 1 Varies with Time. Gels were prepared by heating the solutions about 10 °C above the melting temperature, then kept between 21 and 24 °C. Upon cooling, the clear and fluid solution became opaque and viscous, and gelled after some time.[40] This timing depended on the surfactant chain length and concentration: for 5 and 10 mM solutions of 16-2-16 tartrate, gel formation took place after about 3 and 1 h, respectively, whereas for a 20 mM solution, it took only 10 min. The melting temperature of hydrogels of *n*-2-*n* gemini tartrates with enantiomeric excess (ee) of 1 was measured[41] at 43, 60, and 28 °C for $n = 16$, 18, and 14, respectively.

The details of the morphologies of the gels as a function of time were studied using electron microscopy and are shown in Figure 2. As we previously reported, these gels consist of entangled fibrous structures, typical of physical gels.[42] Images taken at 2 h show some initial ill-defined fibers (Figure 2a). These structures evolve with time and became helical ribbons after around 3 h. The helicity of these ribbons depends on the molecular chirality of tartrate; with L-tartrate, right-handed ribbons were observed, whereas they formed left-handed ribbons with D-tartrate. After about 36 h, helical ribbons closed to form monodisperse tubules, and these tubules are observed with gels

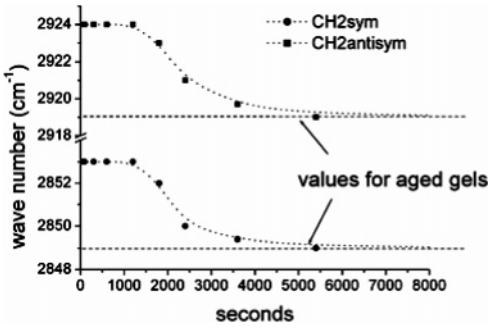

Figure 3. The time evolution of peak positions of CH_2 symmetric and antisymmetric stretching bands of 16-2-16 L-tartrate after dissolution (10 mM solution in H_2O) measured by FT-IR.

aged for more than a year. These results contrast with our initial report that the gels of 16-2-16 tartrate ee 1 consist of twisted ribbons instead of the helical and tubular structures shown in Figure 2. As detailed in the next section, this discrepancy comes from the presence of minute quantities of 16-2-16 Br in the first samples that we prepared with ion exchange column, a technique which does not ensure good stoichiometry.[36]

How does this somewhat slow morphological transition happen? What are the parameters that govern the morphologies? To correlate molecular parameters and supramolecular aggregates' morphology, the organization of alkyl chains was followed as a function of time using FT-IR spectroscopy of the CH_2 antisymmetric and symmetric stretching vibrations (Figure 3). Just after the gel was heated to a clear solution, the position of these bands (2925 and 2853 cm^{-1}, respectively) indicated that the chains were in their melt conformation. The wavenumbers of these bands started to decrease after around 30 min, and kept decreasing for 1.5 h to reach values identical to those observed in aged gels. Note that TEM observations of the morphologies of the self-assemblies show ill-defined fibers for that entire period: the chiral morphologies do not emerge until after 3 h.

Stoichiometry Effect of Residual 16-2-16 Br. As it was mentioned before, it became clear that 16-2-16 tartrate aggregate morphology has a strong dependence on the method used to perform bromide to tartrate ion exchange (twisted ribbons initially observed with ion exchange column or helical ribbons and tubules reported here using silver carbonate). We, therefore, decided to systematically investigate the effect of small amounts of added 16-2-16 Br on the morphology of the chiral ribbons observed with 16-2-16 tartrate. Surprisingly, the addition of a very small amount of 16-2-16 Br dramatically influences the morphologies of the aggregates. In Figure 4, TEM images of the ribbons are shown as a function of the quantity of added 16-2-16 Br. Up to 1 mol % of 16-2-16 Br, tubules were still observed after appropriate aging (see "dimension of the tubules" section). However, one remarkable difference was observed with these samples. At an early stage of gel formation, these ribbons had twisted shapes! After some time, they transformed first to helical ribbons, then to tubules. The twist pitch of these ribbons and the time necessary for the transition from twisted to helical ribbons and to tubules depended strongly on the quantity of 16-2-16 Br: with 1 mol % of 16-2-16 Br, these ribbons remained twisted for as long as 4 days and the apparition of tubules occurred at around 10 days as compared to 3 and 36 h, respectively, in the absence of added bromide. The twist pitch of ribbons with 1 mol % of 16-2-16 Br was about 200 nm.

(39) Valéry, C.; Paternostre, M.; Robert, B.; Gulik-Krzywicki, T.; Narayanan, T.; Dedieu, J.-C.; Keller, G.; Torres, M.-L.; Cherif-Cheikh, R.; Calvo, P.; Artzner, F. *Proc. Natl. Acad. Sci. U.S.A.* **2003**, *100*, 10258.
(40) Gel formation was defined when the solution in a 1 cm tube could be turned upside down without flow.
(41) Melting points of gels were measured by "dropping ball measurements" where a small bead was put on the gel and the temperature increased. The melting point was defined as the temperature at which the bead fell to the bottom of the bottle through the melt gel.
(42) Oda, R. In *Molecular Gels*; Weiss, R. G., Terech, P., Eds.; Springer: The Netherlands, 2006; Chapter 16.

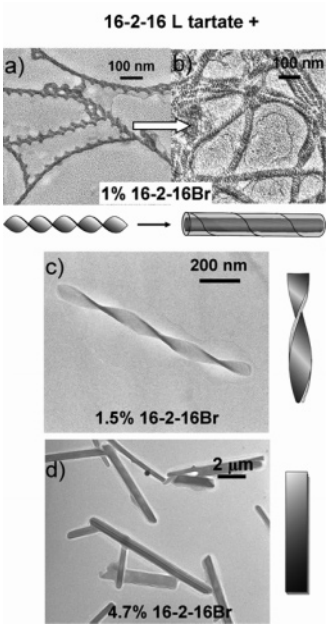

Figure 4. TEM micrographs showing the effect of adding 16-2-16 Br to the morphologies of ribbons formed by 16-2-16 L-tartrate ee 1. (a) With 1% 16-2-16 Br, twisted ribbons transformed into helical ribbons and then into tubules after several days. (b) With 1.5% 16-2-16 Br, only twisted ribbons were observed. (c) Essentially flat ribbons were observed with only 4.7% added 16-2-16 Br.

Quite interestingly, when more than 1.5 mol % of 16-2-16 Br was added, only twisted ribbons were observed, and no tubules were formed even after several months. Also, as the image in Figure 4b shows, the twist pitch was much larger (600 nm). With 4.7% mol % of 16-2-16 Br, essentially unwound, flat, ribbons were observed with occasional twists.

Effect of Enantiomeric Excess. Given the strong perturbation induced by 16-2-16 Br, we speculated that the effect of mixing the opposite 16-2-16 tartrate enantiomer would also be important. In our previous report,[16b] we had shown that the pitch of twisted ribbons decreases continuously as the ee decreases from 1, 0.5, and 0. However, these experiments were performed in the presence of residual 16-2-16 Br, and we did not observe any transition to tubules. Here, we have mixed two pure enantiomers.[43] Gels were prepared in water as described above. TEM observation was performed after 1 month, and the results are shown in Figure 5.

Surprisingly, the tubules exist up to a higher percentage of added opposite enantiomers than in the presence of bromide (Figure 5). When 16-2-16 D-tartrate was added to a solution of 16-2-16 L-tartrate even at 10 mol % (ee 0.8), initially twisted ribbons did transform into helical ribbons and tubules. As when 16-2-16 Br was added, kinetics from twisted ribbons to tubules was significantly slowed by the presence of D-tartrate (3−4 days were needed instead of 36 h). However, when 16-2-16 D-tartrate exceeds 20% (ee < 0.6), only twisted ribbons were observed. The variation of the average twist pitch of the ribbons and their standard deviations as a function of ee is shown in Figure 6.[44] The lower is the ee, the higher is the average pitch and the higher is its polydispersity: for ee $= 0.2$, the twist pitch is 1970

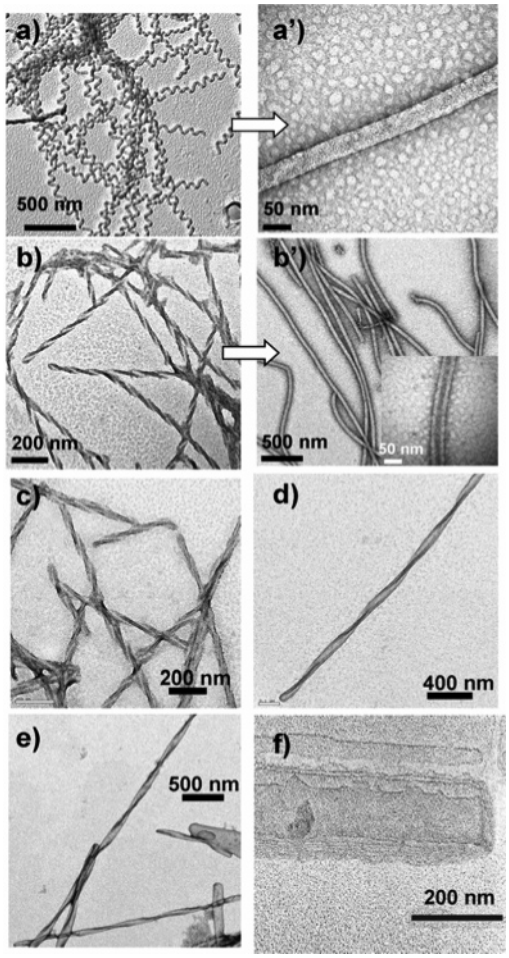

Figure 5. TEM micrographs showing the morphology of ribbons of 16-2-16 tartrate using various enantiomeric excesses. (a) With ee 1, helical ribbons were first observed, which transformed to tubules, whereas (b) with ee 0.8, the ribbons were first twisted, then became helical ribbons, then tubules. Parts c−f show the twisted ribbons observed with ee's of 0.6, 0.4, 0.2, and 0, respectively. The racemic mixture (f) clearly shows a multilayered structure. The twist pitch increases with decreasing ee's.

$\pm$ 840 nm, for ee $= 0.4$, 1580 $\pm$ 330 nm, and for ee $= 0.6$, 500 $\pm$ 50 nm. For ee $= 0.8$ (pitch of 200 $\pm$ 25 nm), measurements were performed on "young" gels, before their transformation to helical ribbons. The twist pitch for ee $= 1$ was measured at 40 °C, where twisted and not helical ribbons are observed (see next section). The pitch value (100 $\pm$ 15 nm) was smaller than what was reported initially[16b] in the presence of residual bromide ions.

Effect of Temperature. After having observed the easiness of transition between twisted and helical/tubular aggregates, it came as a natural question to ask whether temperature had an effect on the morphology of the ribbons. After complete solubilization at 50 °C, the gels of 16-2-16 L-tartrate were kept at several different temperatures below their melting temperature (~43 °C),[45] for a few months. From this test, it was clear that gels kept below 35 °C (Figure 7b) all showed a transition to tubules. On the other hand, the gels between 38 and 40 °C did not show any transition to tubules even after 6 months and remained as twisted ribbons. To rule out possibly very slow transition kinetics at 40 °C, we performed the following test:

(43) The two enantiomers were solubilized together in methanol to form a completely fluid solution. After evaporation of methanol, distilled water was added to prepare the gels.
(44) Statistics were performed with about 50−80 twisted ribbons.
(45) There is a slight variation of gel melting temperature depending on the enantiomeric excess. 43 °C for ee $= 1$ and 46 °C for ee $= 0$.

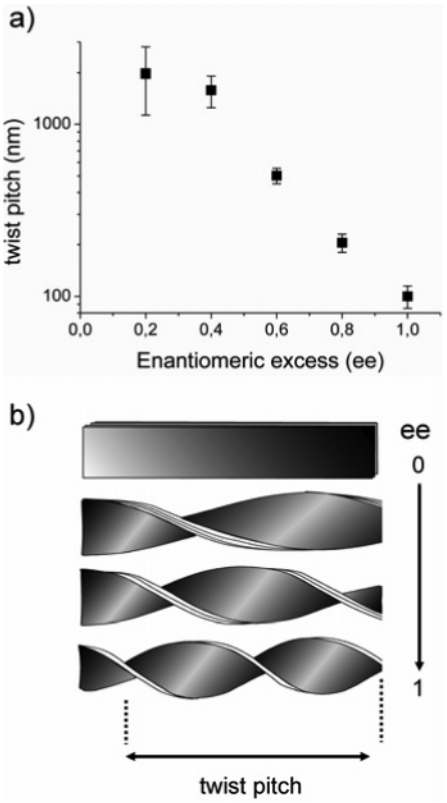

Figure 6. (a) The variation of twist pitch as a function of ee. (b) The twist pitch is defined as a full turn of a ribbon.

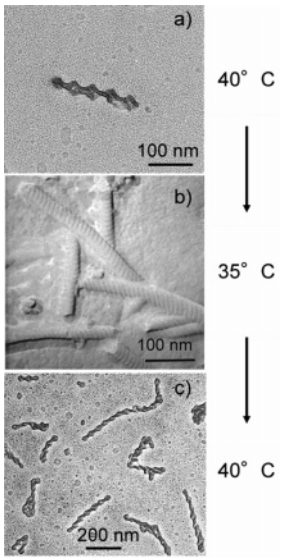

Figure 7. TEM micrographs of gels that were kept at 40 °C (a) show twisted ribbons, whereas those kept at 35 °C (b) or below show a transition to tubules. The tubules can be converted back to twisted ribbons (c), if the gels were kept again at 40 °C.

gels were kept at 35 °C for 1 month, and the presence of tubules was confirmed by TEM. They were then kept at 40 °C for 2 months. These gels showed again twisted ribbons! This clearly indicated that the transition between twisted and helical morphologies of the ribbons is a reversible process. Below 35 °C, tubules are favored, whereas at 40 °C twisted ribbons are favored.

It has been discussed in the literature that the twisted shape of the ribbons can be associated to "fluid membrane" with

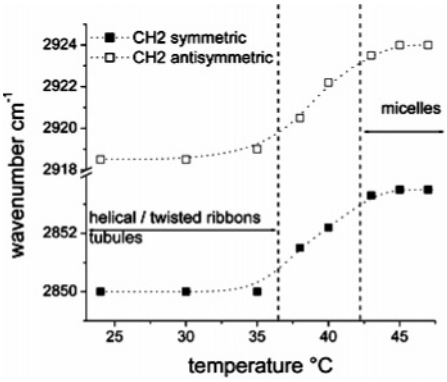

Figure 8. The evolution of peak positions as a function of temperature for CH_2 symmetric and antisymmetric stretching bands for 16-2-16 L-tartrate 10 mM solution measured by FT-IR.

melted chains, whereas the helical ribbons with cylindrical curvature are associated with more rigid membrane with ordered chains.[18−20] To see whether the transition between twisted and helical ribbons observed with 16-2-16 tartrate originates from the organization of hydrophobic chains, we performed FT-IR and X-ray scattering measurements.

For FT-IR measurements, an aged gel of 16-2-16 tartrate ee 1 was heated with a heating rate of about 2 °C per 5 min, and the wavenumbers of CH_2 stretching bands were followed. Figure 8 showed that the wavenumbers of both antisymmetric and symmetric bands increased with temperature. Beyond 43 °C for micellar solutions, they are at their highest values of 2924 and 2853.5 cm^{-1}, respectively, indicating the presence of many gauche conformations and melted chains. On the other hand, below 35 °C, their low values of 2918.5 and 2850 cm^{-1} indicated that the chains were mainly trans conformations. This temperature domain corresponded to the helical ribbons and tubules. In between, the wavenumber showed a continuous increase with temperature. The same low wavenumbers were observed with the ribbons showing twist conformation such as 16-2-16 tartrate ee 1 + 1.5% 16-2-16 Br.

We then performed coupled WAXS/SAXS measurements on the gel as a function of temperature. A gel of 16-2-16 tartrate ee 1 was aged until tubules were formed. The sample was heated from 20 to 50 °C (heating rate of 1 °C/3 min), and data were collected at 1 °C intervals. Next, the temperature was lowered back to 20 °C (interval of 2 °C/3 min), and data were collected at 2 °C intervals. Scattering patterns in Figure 9a (SAXS regime) show broad bands with attenuated cosinus oscillation with the first peak centered at around $q = 0.2$ $Å^{-1}$ at temperatures up to around 42 °C. Such an oscillation indicates interaction between two isolated membrane-type structures and has already been observed in SDS foams.[46] In the WAXS regime shown in parallel in Figure 9b, well-defined peaks indicative of crystalline alkyl chain organization are observed. At higher temperatures, beyond 42 °C, a transition is observed by SAXS, and, simultaneously, the defined peaks in the WAXS domain disappear completely. The transition is reversible upon cooling.

Stacked membranes with a crystalline chain organization are expected to show peaks both at wide angle and small angle as it is observed here at lower temperatures (<42 °C). In contrast, membranes with melted chains are expected to keep a similar

(46) Etrillard, J.; Axelos, M.; Cantat, I.; Artzner, F.; Renault, A.; Weiss, T.; Delannay, R.; Boué, F. *Langmuir* **2005**, *21*, 2229.

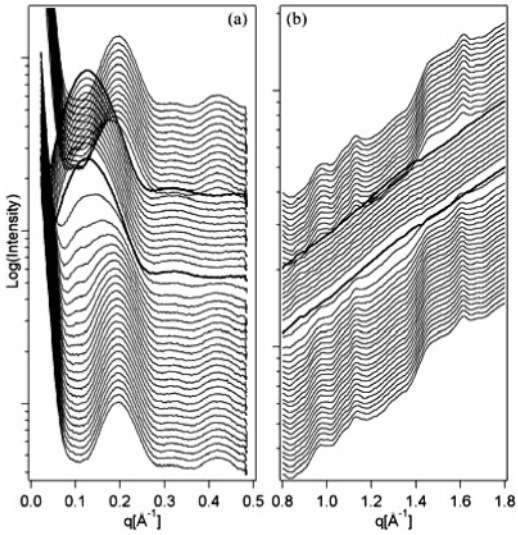

Figure 9. X-ray scattering pattern of 16-2-16 tartrate ee 1 both at SAXS (a) and at WAXS (b) regimes as the gel was heated from 20 °C (bottom) to 50 °C and then cooled back to 20 °C (top). The two bold lines mark the patterns at 43 °C (heating) and 39 °C (cooling). It is clear that the transition happens simultaneously in SAXS and WAXS regimes.

organization at small angle but should not display a well-defined organization at wide angle (representative of alkyl chain organization). For our systems, it is clearly seen that the disappearance of orders at wide angle is concomitant to the disappearance of ordering at small angle, indicating that there is no temperature range in which membrane structure with melted chains exists. Furthermore, for those samples with ee < 0.8, which form only twisted ribbons at room temperature, they also show the same transition where melting of stacked membranes happens at the same time as the disappearing chain ordering (data not shown). Finally, there was no change in the pattern either at small angle or at wide angle regimes before heating and after cooling, whereas once the gels were heated and cooled, the ribbons should not be in their helical form for at least a few hours as it was discussed in the previous section.

These results indicated clearly that the hydrophobic chains of both twisted and helical ribbons have a pseudo-crystalline ordering with mainly trans conformations. This was further confirmed by FTIR measurements showing that the hydrophobic chains of 16-2-16 in gels in twisted ribbons (for example, in gels of 16-2-16 L-tartrate + ϵ16-2-16 Br or + ϵ16-2-16 D-tartrate) did show all trans conformations characterized by low wavenumbers.

Tubules Dimensions. The experiments described above show that 16-2-16 tartrate may form tubules in aqueous solutions even in the presence of small amounts of additives such as bromide ions and the opposite tartrate enantiomer. However, we noticed during these experiments that the diameters of the tubules were not all identical. Although tubule diameter is a key parameter in applications that tubules may have, relatively few reports can be found in terms of the control of the dimension of the tubules.[11,30−32] We investigated in detail the extent to which this parameter can be tuned in our system.

Effect of Additives. In Figure 10, statistics of the diameters of aged tubules are shown for tubules obtained with ee 0.8, ee 1, and ee 1 in the presence of 1% 16-2-16 Br. The addition of 16-2-16 D-tartrate or 16-2-16 Br to 16-2-16 L-tartrate leads to an increase of the tubules' diameter. Specifically, the average

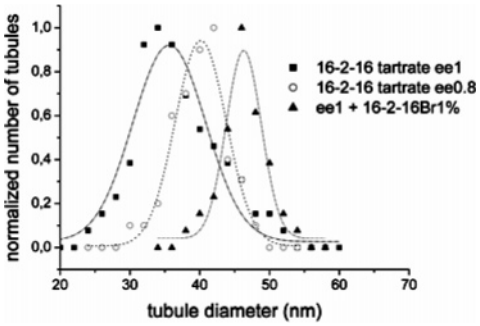

Figure 10. Statistics of tubule diameters for three systems: 16-2-16 L-tartrate ee 1 (distribution over 40 samples), 16-2-16 tartrate ee 0.8 (distribution over 42 samples), and 16-2-16 L-tartrate ee 1 + 1% 16-2-16 Br (distribution over 35 samples).

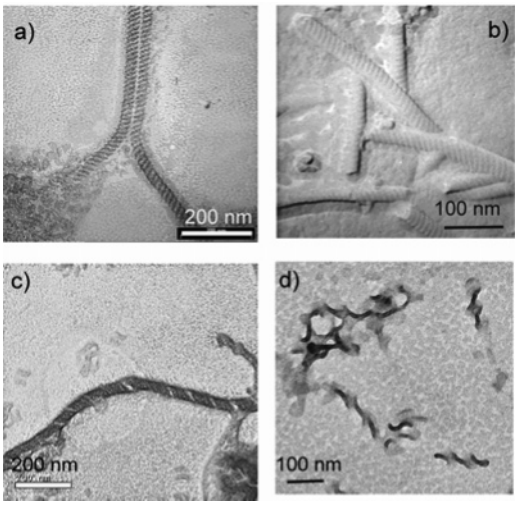

Figure 11. TEM micrographs shown in (a)−(d) show the tubules and ribbons obtained with 14-2-14, 16-2-16, 18-2-18, and 20-2-20 L-tartrate ee 1, respectively. Tubule diameter increases with alkyl chain length. We never observed a transition to tubules with 20-2-20 tartrate.

diameter for 16-2-16 L-tartrate ee 1 was 35.6 ± 5.4 nm, whereas with 10% of 16-2-16 D-tartrate it increased to 40.1 ± 3.7 nm (ee 0.8). Much more striking is the effect of 16-2-16 Br. Only 1% of added 16-2-16 Br increased the diameter of the tubes to 46.3 ± 2.5 nm! Also, it is important to note that the diameter of the tubes is much more homogeneous than the twist pitch of twisted ribbons, which had distributions over a few tens of nanometers.

Effect of Alkyl Chain Length. Tubules were also observed with gemini with other chain lengths than C16: 14-2-14 tartrate ee 1 and 18-2-18 tartrate ee 1.[47] The dimensions of these tubules are dependent on the chain length. For 14-2-14 tartrate, the mean diameter was of the order of 33 ± 4.2 nm,[48] whereas with 18-2-18 tartrate, it was around 48.5 ± 1.2 nm.

Interestingly, samples of 18-2-18 tartrate ee 1 at an early stage of gel formation showed twisted ribbons (Figure 11). The kinetics of transformation to tubules was much slower for 18-

(47) Previously, we reported the presence of helical ribbons for C18 gemini, whereas we did not observe them with C16 gemini.[16b] However, as we have mentioned, it is more likely due to the higher purity of the C18 gemini we have obtained. 12-2-12 tartrate did not form a gel up to a very high concentration, ~40% w/w.

(48) Elemental analysis showed that our samples of 14-2-14 tartrate may not be as pure as those of 16-2-16 and 18-2-18 tartrate. The relatively small difference between 14-2-14 and 16-2-16 as compared to the difference between 16-2-16 and 18-2-18 may come from the possibly larger tubules of 14-2-14 due to the presence of 14-2-14 Br.

2-18 as compared to 16-2-16: about 3−4 days were needed to observe the transition from twisted ribbons to helical ribbons, and about 2 weeks to observe tubules. In the presence of a small quantity of 18-2-18 Br, this transition was as slow as a few months! No such transition was observed with 20-2-20 tartrate ever after 1 year. While we cannot exclude the possibility that long chains intrinsically prohibit the formation of helical ribbons, extremely slow kinetics seems a likely explanation. Along the same line, given that both 18-2-18 and 20-2-20 tartrate form twisted ribbons, and that those of 18-2-18 do transform to tubules with time, it is possible that both 14-2-14 and 16-2-16 tartrate also rapidly go through a twisted ribbons state that we could not observe because of the faster kinetics associated with shorter-chained gemini.

Discussion

Gemini tartrate forms gels in aqueous solutions that consist of multi-layered ribbon-like membranes, which are either twisted or helically coiled. The morphology of these chiral ribbons strongly depends on various physicochemical (external) factors as well as molecular structures. Images from electron microscopy observations reveal that at ee values close to 1 and when the samples are quite pure (less than 1.0 mol % of 16-2-16 Br), twisted ribbons first form that eventually transform to helical ribbons, then to tubules. However, this process is easily disturbed. The transition appears to be prohibited (the ribbons remain twisted) by several parameters such as the presence of added 16-2-16 Br (≥1.5 mol%) or the opposite enantiomer (≥20 mol %), high temperatures, or long (>C20) hydrophobic chains. These observations suggest that the formation of tubules involves a sensitive mechanism with cooperative molecular organization. Interestingly, Br^- anions have a much more drastic effect in prohibiting the transition toward helical ribbons than tartrates of opposite chirality (less than 2 and 10−20 mol %, respectively). While it is difficult to detect 1−2% of residual 16-2-16 Br other than by using elemental analysis, these results underline the importance of the purity of the system and the method used for ion exchange. This much higher sensitivity to the added Br^- than to the added tartrate is probably due to stronger interaction (ion pairing type) between gemini and Br^- than between gemini and tartrate anion as revealed from the Krafft temperature (T_k) and the ionization degree. Indeed, the T_k at 3 mM of 14-2-14 tartrate is 26 °C, whereas it is 32 °C for 14-2-14 Br^-. Also, their ionization degree just above the critical micellar concentration as determined from the conductivity is 0.44 and 0.25, respectively.[49] Both of these results indicate stronger association of Br^- than tartrate[50] with gemini surfactant as it can be seen from the Hofmeister series, [51,52] despite the dianionic character of tartrate. This will probably lead to a stronger effect of nonchiral bomide ions on perturbing chiral assembly morphologies.

The most natural hypothesis to explain the helical to twisted ribbons transformation was a phase transition of alkyl chains between the ordered (trans conformation, Lβ type) and disordered (with a high ratio of gauche conformations, Lα type) state. However, closer investigations revealed that both twisted and helical ribbons appeared only below the Krafft temperature (T_k) of gemini molecules (for C16, $T_k \approx 43$ °C). The chains of gemini molecules in the ribbons are in their ordered phase regardless of their twisted or helical morphologies, that is, even for the conditions under which only twisted ribbons were observed, such as low ee values, more than 2% 16-2-16 Br, or chain length of 20 carbons. WAXS/SAXS measurements also showed the absence of intermediate Lα-type membranes, and, upon heating, a first-order transition from Lβ to micellar phases occurred. FT-IR kinetic measurements show that hydrophobic chains adopt all trans conformations only 1.5 h after cooling the sample, much before the first helical ribbons appear.

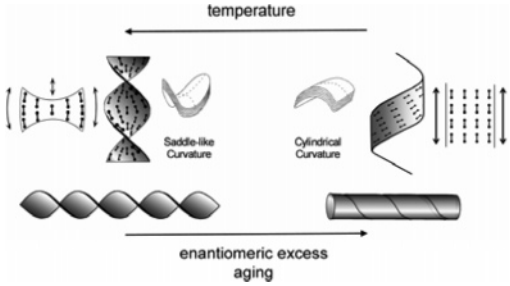

Figure 12. The formation of twisted ribbons with saddle-like curvature requires that the number of molecules per length unit at the edge is higher than that at the center of the ribbons. This was thought to imply greater molecular mobility than in helical ribbons with a cylindrical curvature, which curve without any elongation of the edges.

Contrary to our observations, theoretical considerations suggest that membranes with a real crystalline ordering should not, in principle, allow the saddle-like curvature associated with twisted membranes. As shown schematically in Figure 12, the circumference of twisted ribbons is longer than their length. This can be accommodated by accumulating more molecules per length unit along the edges of the ribbons than in their center, a process apparently compatible only with an Lα-type organization. However, our results do show that transitions between twisted and helical morphologies involve only minor variations of molecular packing within membranes and occur while alkyl chains remain all trans.[53]

As mentioned above, when the systems have high purity and at low temperature, the twisted ribbons of gemini tartrate transform to tubules. The time necessary for this transformation was highly influenced by the "additives factor". For example, as the concentration of added 16-2-16 Br was varied between ~0% and 1%, the time required for the transition to tubules increased from 36 h to 10 days. With the purest samples, likely transient twisted ribbons could not even be detected. This indicates that the formation of tubules is a cooperative process and that its kinetics are extremely sensitive to molecular composition.

If one gives a closer look at the tubules formed with 16-2-16 L-tartrate, we observe that some of these tubules have helical markings whose pitch is much smaller than that of the original ribbon's helical pitch. In fact, we can calculate from the angle of these markings that about three stripes of these markings correspond to the width of the original ribbons. In Figure 13b,

(49) These values were measured with 14-2-14, because the cmc of 16-2-16 is very low, making it difficult to quantitatively determine and compare the ionization degrees.
(50) "Soft" bromide ions have lower hydration energy and higher polarizability, which dominate the dicationic character of tartrate with "hard" carboxylate ions. It is interesting to note that the cmc of gemini (14-2-14) tartrate (6.4×10^{-5} mol/L) is lower than that of gemini (14-2-14) Br. In this case, it is the capacity of tartrate to form intermolecular hydrogen bonds at the micellar surface that cooperatively favors the micellar formation.
(51) Hofmeister, F. *Arch. Exp. Pathol. Parmakol.* **1888**, *24*, 247−260.
(52) Romsted, L. *Langmuir* **2007**, *23*, 414−424 and references therein.
(53) The detailed study on the molecular organization of these fibers is not in the scope of this Article and will be presented elsewhere.

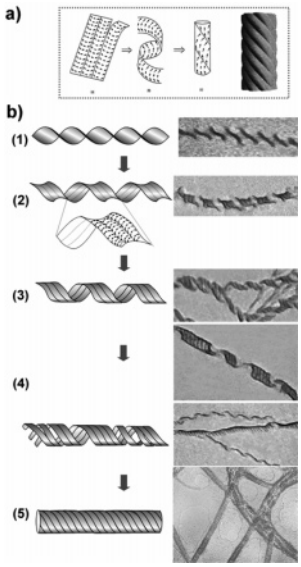

Figure 13. (a) The model proposed by Selinger et al.[54] giving rise to ripples due to the modulation in the tilt direction separated by sharp domain walls. (b) Transition from twisted ribbons to helical ribbons, and then to tubules observed with 16-2-16 L-tartrate ee 1 with 1% 16-2-16 Br. Ripples appear together with helical ribbons (in b(2)).

some examples of the intermediate state of the ribbons that we observed are shown. These images seem to confirm that the stripes appear at the same time when the twisted ribbons transform to helical ribbons, much before closing to form tubules.

What is the origin of these stripes? To understand this, we may call for a previous report by Selinger et al.[54] where the authors had predicted the presence of ripples due to the modulation in the tilt direction of molecules respective to their neighbors separated by sharp domain walls giving an undulated and twisted tubular structure as shown in Figure 13a. In our case, the image in Figure 13b(2) suggests that the original twisted ribbons are made of about three stripes instead of each stripe making a helical ribbon as proposed in Figure 13a. Thus, helical ribbons form with three stripes, which then close to form tubules. Once the tubules are formed, it even seems that they can break up at any ripple position as it is seen in Figure 13b(4).

In a similar way, as it was possible to tune the morphology of the chiral ribbons in terms of helical versus twisted morphology and in terms of the twist pitches of the ribbons, it was also possible to tune the diameters of the tubules. Here again, the same factors as above play important roles. The diameters varied from 33 to 48 nm when the chain length of gemini molecules increased from C14 to C18. This may be attributed to a decrease in tubule curvature due to the rigidification of the membranes with longer chains. Addition of 10 mol % of the opposite enantiomer leads to a 15% increase in tubule diameter, while only 1% of added gemini bromide increased the tubule diameter by 30%!

Such a control over the tubule diameter is apparently closely related to the fine variation of molecular organization in the course of tubule formation.

Conclusion

The morphology of chiral ribbons obtained with gemini tartrate strongly depends on various physicochemical (external) factors as well as on molecular structure. As solutions of gemini tartrate ee 1 are cooled from above 45 °C to room temperature, they form helical ribbons that close to form tubules. When the system contained a small amount of 16-2-16 Br or of the opposite enantiomers, twisted ribbons are first observed, which slowly transform to helical ribbons, then to tubules. This transformation takes more or less time depending on the chain length and the quantity of additives. The transition to helical ribbons was easily prohibited when the concentration of additives was further increased. Temperature is also a determining factor of aggregate morphology. At a low temperature, a transition to tubules is observed, whereas within a narrow temperature range just below the transition to micellar solution, tubules transform to ribbons with a twisted shape. Such a dynamic transition behavior had never been observed before! Detailed examinations by FT-IR or X-ray scattering indicated that the level of gauche conformation is extremely low regardless of the ribbons morphology and the Lβ-type lamellae to micelle transition is a first-order transition. This excluded the presence of Lα-type lamellar phase. Therefore, the transition between helical and twisted ribbons is not directly related to the ordered to disordered phase of the hydrophobic chains. The extremely high sensitivity of the morphology of the ribbons to external and molecular factors allowed us also to easily tune the diameters of these nanometric tubules. Along with the somewhat more predictable effect of chain length, the possibility of increasing the tubular diameters by simply adding the same amphiphiles with bromide counterions provides a unique approach for controlling the morphology of supramolecular chiral objects.

Acknowledgment. This work was supported by the Centre National de la Recherche Scientifique (CNRS), the University of Bordeaux I, and the Conseil Régional d'Aquitaine. We thank F. MacKintosh for useful discussions on ribbons morphology, S. Manet for her suggestions on cation−anion interaction, and T. Buffeteau for useful suggestions on FTIR spectroscopy.

JA0682172

(54) Selinger, J. V.; MacKintosh, F.; Schnur, J. *Phys. Rev. E* **1996**, *53*, 3804.